JOM, Vol. 70, No. 6, 2018
https://doi.org/10.1007/s11837-018-2852-x

Effects of Testing Method on Stretch-Flangeability of Dual-Phase 980/1180 Steel Grades

MYKAL MADRID,[1,5] CHESTER J.VAN TYNE,[1,2] SRIRAM SADAGOPAN,[3] ERIK J. PAVLINA,[4] JUN HU,[4] and KESTER D. CLARKE[1]

1.—Colorado School of Mines, 1500 Illinois St., Golden, CO 80401, USA. 2.—Virginia Tech, 445 Old Turner St., Blacksburg, VA 24061, USA. 3.—ArcelorMittal, 3001 E. Columbus Dr., E., Chicago, IN 46312, USA. 4.—AK Steel Research and Innovation Center, 6180 Research Way, Middletown, OH 45005, USA. 5.—e-mail: mmadrid@mines.edu

Challenging fuel economy and safety standards in the automotive industry have led to the need for materials with higher strength while maintaining levels of formability that meet component manufacturing requirements. Advanced high-strength steels, such as dual-phase steels with tensile strengths of 980 MPa and 1180 MPa, are of interest to address this need. Increasing the strength of these materials typically comes at the expense of ductility, which may result in problems when stamping parts with trimmed or sheared edges, as cracking at the sheared edge may occur at lower strains. Here, hole expansion tests were performed with different punch geometries (conical and flat-bottom) and different edge conditions (sheared and machined) to understand the effects of testing conditions on performance, and these results are discussed in terms of mechanical properties and microstructures.

INTRODUCTION

Challenging fuel economy and safety standards[1,2] in the automotive industry have led to the need for materials with higher strength while maintaining levels of formability that meet component manufacturing requirements. Advanced high-strength steels (AHSS), which include dual-phase (DP) steels, are of interest due to their excellent mechanical properties (for example, high initial work hardening rate and high tensile strength to yield strength ratio). DP steels typically consist of a relatively soft ferrite matrix and islands of hard martensite,[3] with strength increasing with increasing volume fractions of martensite. Lower-strength DP steels have been implemented in a number of vehicles, though higher-strength levels are desired and require further investigation.[2] Higher strength generally comes at the expense of ductility, which becomes a particular challenge when stamping parts with trimmed or sheared edges, as the parts may experience cracking at the sheared edge even at relatively small strains. Stretch-flangeability, measured by hole expansion testing (HET), is a measure of formability that has been used to characterize the performance of materials during forming of sheets with holes.[4–17]

HET can be performed with conical[4–8] and flat-bottom punches,[4,9–13] as well as different hole preparation methods (for example, sheared or machined).[4,14–16] Studies have shown that materials tested with a conical punch generally have a higher hole expansion ratio (HER) than the same material tested with a flat-bottom punch.[4,12,18–20] This difference has been attributed to the bending component introduced by the conical punch creating a material constraint that delays failure.[20] Edge conditions have also been shown to affect HER, with machined edges having a higher HER than sheared edges.[14] This effect is because shearing creates a work-hardened zone at the edge of the material, which acts as a stress concentrator, and may result in pre-initiated damage—voids or cracks—at the sheared edge.[4] Further investigation is needed of HER obtained with a flat-bottom punch and different edge conditions, since limited results have been presented in the literature to date.[4,9,12,13]

Microstructural characteristics such as martensite volume fraction (MVF) and martensite morphology in the DP steels have an effect on stretch-flangeability.[4–7,17,21] Many studies have reported that the difference in hardness between ferrite and martensite in a DP microstructure was a dominant

(Published online April 10, 2018)

factor in stretch-flangeability.[5,6,9] HER tends to increase as the relative strength difference between the ferrite and martensite decreases or as the microstructural homogeneity increases. Hasegawa et al.[5] reported that increasing MVF resulted in a higher HER and that single-phase martensitic sheets showed the highest HER. Other reports have shown the opposite trend, though the materials in one report[6] had different mechanical properties and morphologies for the same steel grade, while the other report[10] focused more on the growth of epitaxial ferrite and its effect on HER.

Martensite morphology also has an effect on formability. Kim et al.,[17] examined the morphological differences between the DP steels studied by Hasegawa et al. and concluded that, in the higher MVF steel which showed a martensite network surrounding ferrite, the martensite takes on more of the plastic deformation than the ferrite, delaying failure. The martensite network surrounding the ferrite has been shown to prevent crack propagation at the martensite–ferrite interface, which improves stretch-flangeability.[21] Terrazas et al. took a different approach and characterized the martensite dispersion through the area density of martensite colonies.[6] They concluded that HER increases with the increasing number of evenly dispersed martensite colonies per unit area, an indication of the homogeneity in the microstructure, since fine and evenly dispersed martensite colonies provide more obstacles for crack propagation.[6]

Generally, there have been few studies on HER of DP steels with tensile strengths of 1180 MPa,[6] and none have reported results from 1180 alloys with microstructures consisting of more than 50% martensite, or across a range of testing conditions. This report focuses on the effects of the HET type and how microstructure may affect the HER of DP 980/1180 steel grades.

PROCEDURE

The nominally 1.4-mm-thick uncoated sheet DP 980 (0.09C-2.1Mn wt.%) and DP 1180 (0.13C-2.24Mn wt.%) materials were used in this experiment. Standard light optical and scanning electron microscope (SEM) techniques were used to characterize the microstructures. The MVF for the DP steels was calculated using the point counting method, with concentric circles on SEM images of the samples in the planar orientation.[22] A total of 10 SEM micrographs at ×3000 magnification were used for analysis. The martensite carbon content was calculated assuming that all bulk carbon is in the martensite:

$$C_{\alpha'} = C_{\text{bulk}}/\text{MVF} \tag{1}$$

where $C_{\alpha'}$ is the martensite carbon content in wt.% and C_{bulk} is the carbon content of the steel in wt.%.[6]

Mechanical properties were determined by uniaxial tensile testing according to ASTM E8. The average of four samples tested along the rolling direction are reported. The strain-hardening exponent, n, was calculated from a true strain of 0.02 up to the strain at ultimate tensile stress. The normal anisotropy coefficient, R_{m}, was determined for samples pre-strained to 4.5% engineering strain.

HET was performed according to ISO 16630 and the configuration is shown in Refs. 23 and 24. Two types of edge conditions (sheared and machined) and punch geometries (conical and 25.4 mm flat-bottom) were tested. The nomenclature for the testing conditions is conical punch/machined edge (CM), conical punch/sheared edge (CS), flat punch/machined edge (FM), and flat punch/sheared edge (FS). Sheared edges were created using a punch and die set with a clearance of 11% of the material thickness, and all samples were tested with the burr away from the punch side of the sheet. Blanks of 101.6 × 101.6 mm and 177.8 × 177.8 mm in size with a 10-mm hole were tested at a punch speed of 0.5 mm/s and with a camera system capturing visual data during the test. Once a through-thickness crack was observed by the user, the test was stopped and post-processing was performed in ImageJ.[25] The HER is calculated as follows,

$$\text{HER} = \frac{D_{\text{f}} - D_{\text{o}}}{D_{\text{o}}} \times 100 \tag{2}$$

where D_{o} is the initial hole diameter and D_{f} is the hole diameter at the time a crack is first observed. To determine whether the crack initiated along the rolling direction, crosshairs were placed through the center of the test sample in ImageJ, and cracks oriented less than or equal to 30° from the center in either direction, were considered to have initiated along the rolling direction.

RESULTS

Microstructures

Figure 1 shows secondary electron images for DP 980 (1a) and DP 1180 (1b) showing microstructures consisting of martensite (lighter regions) and ferrite (darker regions). The DP 980 shows equiaxed ferrite grains with a martensite network along the ferrite grain boundaries, along with some martensite islands within the ferrite grains. The microstructure of the DP 1180 shows a martensite matrix with ferrite islands similar to Kim et al.[17] The MVF's were measured to be 52 ± 6% and 66 ± 5% for DP 980 and DP 1180, respectively. Figure 2 shows light optical images of the microstructural banding in both steel grades. Microstructural banding has been shown to effect mechanical properties and fracture characteristics by creating void nucleation sites.[26]

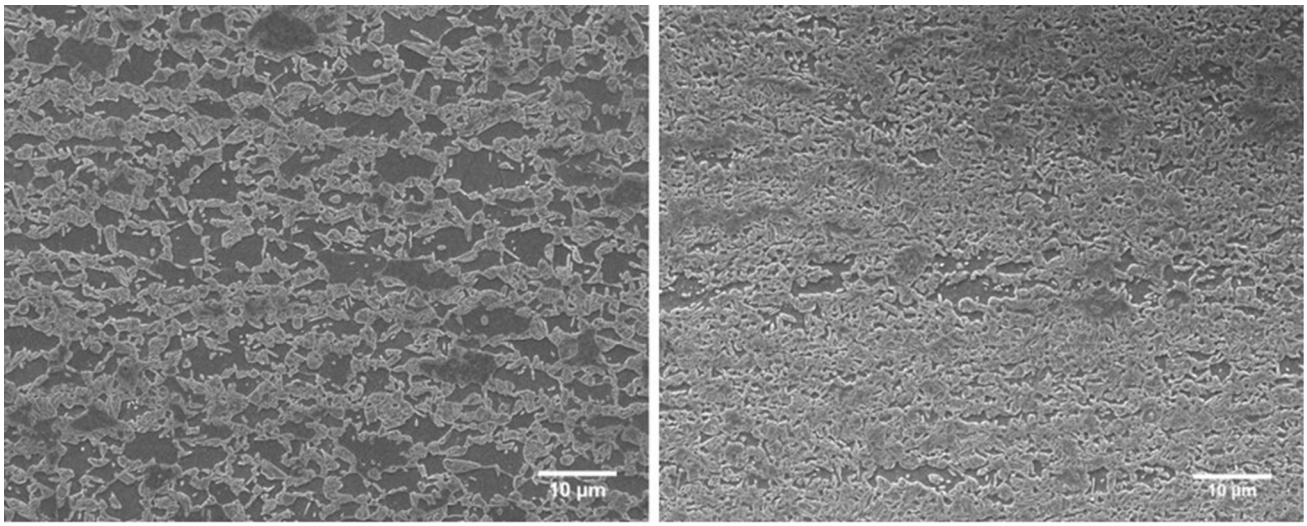

Fig. 1. Secondary electron images of (a) DP 980 and (b) DP 1180. Longitudinal sections with the rolling direction horizontal. The samples were etched with 2% Nital.

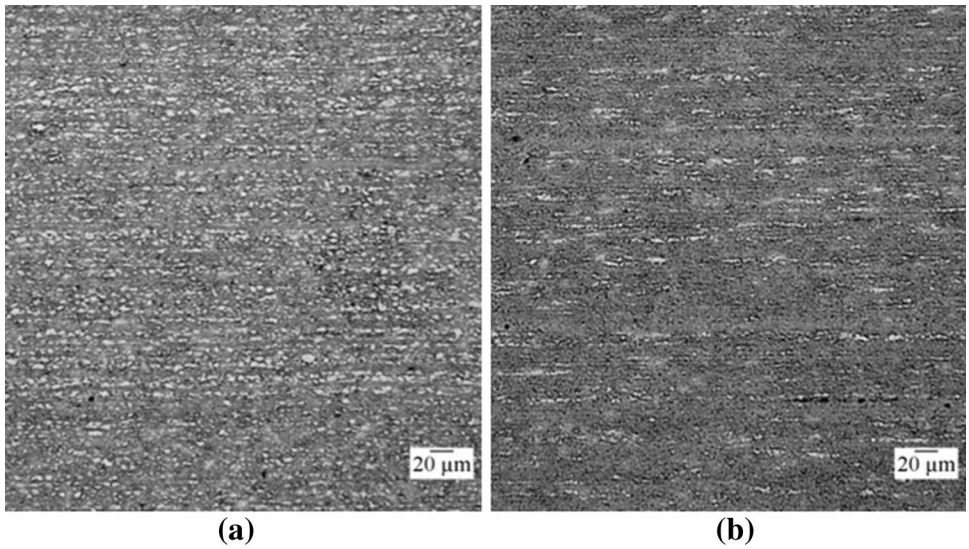

Fig. 2. Light optical images of (a) DP 980 and (b) DP 1180. Longitudinal sections with the rolling direction horizontal showing microstructural banding. The samples were etched with 2% Nital.

Mechanical Properties

Table I details the measured mechanical properties of the DP steels. The yield strength (YS) and the ultimate tensile strength (UTS) correlate as expected with increasing MVF.[27] The elongation of the DP 1180 is somewhat lower than the DP 980, and the strain-hardening exponent (n), normal anisotropy coefficient (R_m), and YS to UTS ratio (YS:UTS) are similar. The reduction of area (ROA) in the DP 980 is slightly higher than the DP 1180.

Hole Expansion Ratio

Figure 3 shows the HER of the DP steels as a function of edge condition and punch geometry, and relates HER with martensite carbon content. Overall, DP 980 has a higher HER than DP 1180 independent of edge condition or punch geometry. Between the two test geometry conditions, results show that the conical punch has a higher HER than a flat-bottom punch for the same edge conditions. The machined edge also has a higher HER than the

Table I. Mechanical properties for DP 980 and DP 1180

Material	YS (MPa)	UTS (MPa)	TE (MPa)	n	R_m	YS:UTS	ROA	Martensite carbon content (wt.%)
DP 980	716 ± 33	1043 ± 15	13.8 ± 0.3	0.11	0.89	0.69	36.5 ± 0.8	0.17
DP 1180	827 ± 5	1256 ± 3	9.9 ± 0.7	0.10	0.88	0.66	32.5 ± 2.3	0.20

sheared edge for the conical punch, though this trend is not seen with the flat-bottom punch. The ratios shown in Fig. 3 were calculated between the two materials for a given test condition.

DISCUSSION

Effects of Edge Conditions and Punch Geometry on HER

The hole preparation method has shown to play a significant role on the HER.[4,14–16] Generally, sheared holes lead to a lower HER than machined holes due to the reduced ductility of the work-hardened shear-affected zone and the possibility of pre-initiated voids or cracks at the sheared edge.[4] A machined hole removes the shear-affected zone, generally resulting in improved HER.[14] In this study, the CM samples showed a higher HER than the CS samples for a given material in agreement with the literature. However, the HER of the FM samples were nearly identical to the FS samples despite edge condition differences, which is in agreement with work carried out by Pathak et al., which concluded that samples (DP 600 and complex phase 590 steel) run with a flat-bottom punch were not sensitive to edge conditions, and this was attributed to the fact that stress state is different, causing failure to occur away from the hole edge.[4]

The punch geometry also has an effect on the HER. Stanton et al.[12] performed HET on various aluminum alloys using both a flat-bottom and conical punch with different edge conditions, concluding that the conical punch generally produced higher HER than the flat-bottom punch.[4,12,18,19] In HET, the flat-bottom punch causes the sheet edge to undergo stretching, while the conical punch causes both stretching and bending, and Neuhauser et al.[20] explained that bending in a stretch bend test creates a material constraint that delays failure. The bending component creates a strain gradient in the material with the highest strains at the outer surface (at the burr). In this study, the CM samples had a higher HER than the FM samples and the CS samples performed better than the FS samples for a given material.

HER results show that the testing conditions follow common trends seen in the literature. The FM condition differs from the other testing conditions in that there is no strain gradient in the material induced by the punch geometry and no strain hardening at the edge of the sample hole due to the hole preparation method. There is limited literature published for HET with a flat-bottom punch with varying edge conditions, and, specifically, on AHSS[4,9–11,13] that have similar mechanical properties as the steels in this study.

It is interesting to note that the ratios of HET for DP 980 and DP 1180 shown in Fig. 3 are independent of test conditions (i.e., punch geometry and edge condition) with the exception of the FM samples. Based on these results, it is suggested that HET performed with the CS, CM, and FS test conditions result in similar relative HER values for two sheets with similar n, R_m, and YS:UTS (see Table I).

DP 1180 grades are fairly new and still being evaluated for specific applications in structures, but, in this case, the material tested seems to have a HER performance that might be expected relative to the tested DP 980 sheets (i.e., somewhat lower HER due to decreased tensile ductility as a function of the increased strength). HER performance of DP 1180 grades does not increase with MVF relative to DP 980 in this case, suggesting that the reported correlation between MVF and HER does not apply at these strength levels.[5] The present results also specifically suggest that the FM test condition may result in different relative HER results for materials that have similar HER values under CS, CM, and FS test conditions.

Microstructure and HER

The mechanical properties that have been reported[7,28,29] to contribute to HER (n, R_m, and YS:UTS) are approximately equal for the two steels tested; however, the ROAs are slightly different. Pathak et al. concluded that increasing ROA results in higher HER, which is in agreement with this study. The effects of microstructure on HER between the two steels tested, particularly MVF, martensite carbon content, and martensite morphology, are considered. As previously mentioned, the literature has shown opposing trends for MVF and HER.[4–6,10] However, most current studies only report results for MVFs up to 50%, or for a fully martensitic alloy.[5–7,10,17] The MVFs for the two sheets tested here lie between those values, and the results showed that, as the MVF increased, the HER decreased.

The difference in hardness between martensite and ferrite has also been shown to correlate well with HER,[5,6,9] because strain localization to the ferrite by the surrounding martensite is reduced as martensite hardness decreases. The results of this

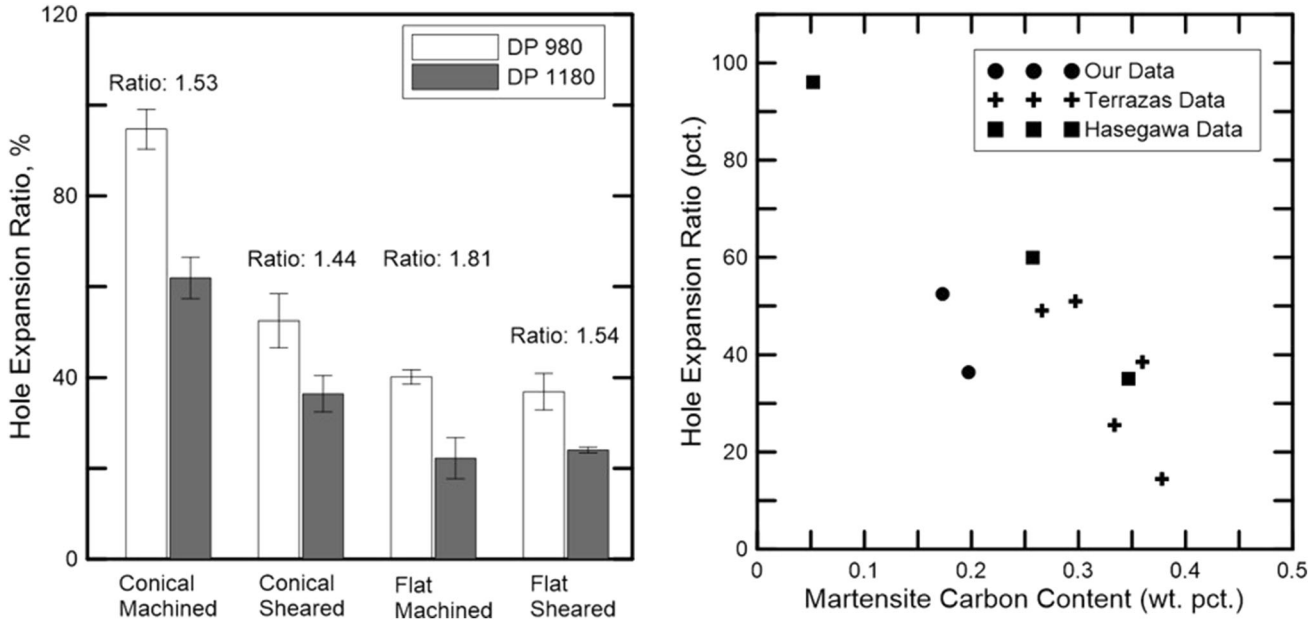

Fig. 3. Hole expansion ratios for DP 980 and DP 1180 as a function of punch geometry and edge conditions and the hole expansion ratio as a function of martensite carbon content.

study show that the HER decreases as martensite carbon content increases from the DP 980 to the DP 1180, as shown in Fig. 3.

Martensite morphologies such as interconnected martensite have been shown to have an effect on HER.[17,21] Interconnected martensite has been shown to result in improved HER as the martensite takes on most of the plastic deformation shielding the ferrite and delaying failure.[17,21] Here, the DP 980 microstructure consists of an equiaxed microstructure with martensite networks along the ferrite grain boundaries, while the DP 1180 has sufficiently high MVF that the microstructure is more aptly described as ferrite islands in a martensite matrix.

In this study, the HER decreased as the MVF increased and the martensite carbon content increased. There are limited HER results that have been reported for alloys at the strength levels and martensite volume fractions of the materials examined here, but increasing MVF appears to result in a decrease in HER. In order to quantify the effect that MVF has on HER, a broader range of DP steels with MVFs between 70% and 100% and microstructure morphologies need to be tested. Based on our results and data from other studies,[5,7,17] there may be a peak in the HER at MVF values around 50%, suggesting that martensite morphology may affect HER more at higher MVFs.

The morphology and MVF are dependent on one another, and it would be useful to perform further experiments in the areas where morphology may be the driving force for HER to better understand crack initiation and propagation, which would help to design microstructures for increased AHSS formability.

CONCLUSION

The test factors affecting HER in a DP 980 and a DP 1180 sheet of the same thickness including punch geometry and the hole edge condition were analyzed through HET. It was found that machined edges have a higher HER than sheared edges for the conical punch, but the trend is not seen with the flat-bottom punch. The conical punch geometry showed a higher HER than the flat-bottom punch for all testing conditions. It is interesting to note that the relative HER for the CS, CM, and FS test configurations result in the same ratio for both materials, even though the strength levels and microstructure vary significantly. For the FM condition, however, the HER results did not follow the relative trends observed in other geometries, suggesting the factors controlling HER in this test geometry are different, at least for the steels tested.

The effect of microstructure on stretch-flangeability was also analyzed through microstructural analysis and HET. Two DP steels with similar mechanical properties, different MVF, martensite carbon contents, and morphologies were analyzed for their effect on HER and overall formability. Increasing MVF and martensite carbon content was found to decrease HER, which may be expected based solely on strength level and tensile ductility. The microstructural morphology that appears to improve formability consisted of a martensite network along ferrite grain boundaries, although higher-strength DP alloys will require martensite fractions that may preclude this morphology. It was concluded that the martensite carbon content, volume fraction, and morphology all play a role in

formability up to a given value of MVF, above which the martensite morphology may have the greatest effect.

ACKNOWLEDGEMENTS

Baosteel are acknowledged for providing the experimental material. Hole expansion testing was performed at ArcelorMittal (East Chicago) and AK Steel (Middletown, OH). Dr. Kavesary Raghavan and Dr. Mai Huang are acknowledged for assisting with the testing. The sponsors of the Advanced Steel Processing and Products Research Center at Colorado School of Mines are gratefully acknowledged for their support and funding.

REFERENCES

1. United States Department of Transporation, "Corporate Average Fuel Economy". http://www.nhtsa.gov/laws-regulations/corporate-average-fuel-economy. Accessed 25 January 2017.
2. O. Bouaziz, H. Zurob, and M. Huang, *Steel Res. Int.* 84, 937 (2013).
3. M.Y. Demeri, *ASM Handbook*, vol. 14B (Materials Park: ASM International, 1996), p. 530.
4. N. Pathak, C. Butcher, and M. Worswick, *J. Mater. Eng. Perform.* 25, 4919 (2016).
5. K. Hasegawa, K. Kawamura, T. Urabe, and Y. Hosoya, *ISIJ Int.* 44, 603 (2004).
6. O. Terrazas, K.O. Findley, and C.J. Van Tyne, *ISIJ Int.* 57, 937 (2017).
7. X. Chen, H. Jiang, Z. Cui, C. Lian, and C. Lu, *Proc. Eng.* 81, 718 (2014).
8. K. Mori, Y. Abe, and Y. Suzui, *J. Mater. Process. Technol.* 210, 653 (2010).
9. M.D. Taylor, K.S. Choi, X. Sun, D.K. Matlock, C.E. Packard, L. Xu, and F. Barlat, *Mater. Sci. Eng. A* 597, 431 (2014).
10. J. Lee, S. Lee, and B.C. De Cooman, *Mater. Sci. Eng. A* 536, 231 (2012).
11. P. Tsipouridis, E. Werner, C. Krempaszky, and E. Tragl, *Steel Res. Int.* 77, 654 (2006).
12. M. Stanton, R. Bhattacharya, I. Dargue, R. Aylmore, and G. Williams, *AIP Conf. Proc.* 1353, 1488 (2011).
13. D.J. Thomas, *J. Fail. Anal. Preven.* 13, 451 (2013).
14. A. Karelova, C. Krempaszky, E. Werner, P. Tsipouridis, T. Hebesberger, and A. Pichler, *Steel Res. Int.* 80, 71 (2009).
15. R.J. Comstock Jr, D.K. Scherrer, and R.D. Adamczyk, *J. Mater. Eng. Perform.* 15, 675 (2006).
16. B.S. Levy, M. Gibbs, and C.J. Van Tyne, *Metall. Mater. Trans. A* 44A, 3635 (2013).
17. J.H. Kim, M.G. Lee, D. Kim, D.K. Matlock, and R.H. Wagoner, *Mater. Sci. Eng. A* 527, 7353 (2010).
18. P. Larour, J. Freudenthaler, A. Grunsteidl, and K. Wang, *IDDRG Conf. Proc.* 188 (2014).
19. E. Iizuka, M. Urabe, Y. Yamasaki, and J. Hiramoto, *Phys.: Conf. Ser.* 896, 012008 (2017).
20. F.M. Neuhauser, O.R. Terrazas, N. Manopulo, P. Hora, and C.J. Van Tyne, *IOP Conf. Ser.: Mater. Sci. Eng.* 159, 012011 (2016).
21. M. Miura, M. Nakaya, and Y. Mukai, "Cold-rolled, 980 MPa Grade Steel-sheets with Excellent Elongation and Stretch-flangeability," http://www.kobelco.co.jp/english//ktr/pdf/ktr_28/008-012.pdf. Accessed 15 Dec 2017.
22. ASTM E562-11, Standard Test Method for Determining Volume Fraction by Systematic Manual Point Count (2011).
23. M. Madrid, C.J. Van Tyne, and K. Clarke, in *MS&T conference proceedings* (2017), p. 1302.
24. H. Shih and M. Shi, *J. Manuf. Sci. Eng.* 133, 061018 (2011).
25. J. Schindelin, I. Arganda-Carreras, and E. Frise, *Nat. Methods* 9, 676 (2012).
26. G. Avramovic-Cingara, C.A.R. Saleh, M.K. Jain, and D.S. Wilkinson, *Metall. Mater. Trans. A* 40A, 3117 (2009).
27. R. Davies, *Metall. Mater. Trans. A* 9, 671 (1978).
28. S. Sadagopan and D. Urban, Formability Characterization of a New Generation of High Strength Steels. http://www.steeltrp.com/finalreports/finalreports/0012NonPropFinalReport.pdf Accessed 14 Nov 2017.
29. X. Jin, L. Want, and J.G. Speer, in *ISAS 2013* (2013), p. 60.